Hydrogen Bonding to Multifunctional Molecules: Spectroscopic and ab Initio Investigation of Water Complexes of Fluorophenylacetylenes

Surajit Maity and G. Naresh Patwari*

Department of Chemistry, Indian Institute of Technology Bombay, Powai, Mumbai 400076, India

Received: October 15, 2008; Revised Manuscript Received: December 19, 2008

The water complexes of 4-fluorophenylacetylene and 2-fluorophenylacetylene were investigated using IR-UV double resonance spectroscopy. Both 4-fluoro- and 2-fluorophenylacetylenes form a cyclic complex with water incorporating C−H···O and O−H···π hydrogen bonds. These structures are similar to the phenylacetylene−water complex, implying that the fluorine substitution on phenylacetylene does not alter the intermolecular structure. Further, the presence of fluorine enhances the interaction of water with the acetylenic π electron density. This behavior of fluorophenylacetylenes is dramatically different from that of fluorobenzene and fluorostyrene. A second water complex was also observed in the case of 2-fluorophenylacetylene in which water interacts with fluorine atom and acetylenic C−C triple bond in a double-donor fashion. Additionally, two distinct 2-fluorophenylacetylene−$(water)_2$ complexes were also observed. The first is a cyclic complex in which two water molecules bridge the hydrogen bond donor and acceptor sites present in 2-fluorophenylacetylene. The second is a kinetically trapped higher energy structure in which one water molecule acts as a double-acceptor.

1. Introduction

The majority of hydrogen bonding observed in both the gas and the condensed phases can be summarized using Etter rules.[1] In addition, on the basis of the geometries of several mixed dimers obtained using rotationally resolved spectroscopy, Legon and Millen laid down rules for formation of X−H···B hydrogen bonding.[2] Both the Etter and the Legon−Millen rules govern the hierarchy of hydrogen bond formation. The Etter rules, in particular, have been consistently used to predict the formation of supramolecular synthons and thus form guidelines for crystal engineering. However, exceptions to Etter rules have been reported, and these exceptions mostly pertain to hydrogen-bonding patterns observed in multifunctional molecules.[3] One of the major challenges that needs to be addressed in hydrogen bonding is to know, a priori, how the individual functional groups in multifunctional molecules will behave when they are made to interact with suitable hydrogen-bonding partners. In multifunctional molecules, the exact hydrogen bonding pattern will be a result of subtle competition between various possibilities. Toward the goal of comprehending the hydrogen-bonding behavior of multifunctional molecules, we had earlier investigated hydrogen-bonded complexes of phenylacetylene with various solvent molecules such as water, methanol, ethanol, ammonia, alcohols, and amines.[4] The hydrogen-bonded complexes of phenylacetylene form a wide variety of intermolecular structures, which stem out of a subtle balance of intermolecular forces in various possible intermolecular structures. For instance, phenylacetylene forms a cyclic complex with water incorporating O−H···π and C−H···O hydrogen bonds, the structure of which is different from both the benzene−water and acetylene−water complexes, even though phenylacetylene incorporated the features of both benzene and acetylene.[4a] Because phenylacetylene consists of only π-bonding electrons (benzene ring and acetylenic C−C triple bond), the hierarchy of hydrogen bond accepting sites cannot be determined on the basis of either Etter or Legon−Millen rules. Further, it was also observed that even minimal changes in the interacting partners, such as substitution by a ubiquitous methyl group, can result in dramatic change in the intermolecular structure.[4]

Substitution of fluorine on the benzene ring of phenylacetylene increases the number of possible hydrogen-bonding sites. Singly fluoro-substituted phenylacetylenes have four hydrogen-bonding sites in the form of benzene ring and the acetylene moiety, which can act as π acceptors, fluorine as a σ acceptor, and the relatively acidic acetylenic C−H group, which can act as a σ donor. Apart from addition of an extra hydrogen-bond acceptor site in the form of lone pair electrons of fluorine atom, substitution with fluorine atom also will lead to changes in the π electron densities of benzene ring and acetylenic C−C triple bond and also can affect the acidity of the acetylenic C−H group.[5] Thus, the substitution with fluorine is expected to alter the binding energies along various minima on the intermolecular potential and therefore will lead to the modification of relative hydrogen-bonding affinities of various sites. In this article, we present the spectroscopic and ab initio investigations carried out on water complexes of 4-fluorophenylacetylene (4FPHA) and 2-fluorophenylacetylene (2FPHA). The primary motivation for this investigation was to determine the effect of substitution with fluorine on phenylacetylene (PHA) on the intermolecular structure upon interaction with water. We address here whether the water will switch from π hydrogen binding at the acetylenic C−C triple bond site to σ hydrogen bonding at the fluorine site. This can be viewed as a test case for the Legon−Millen rules,[2] wherein the relative affinity of hydrogen bonding of π and σ acceptors can be evaluated, a factor that was missing in phenylacetylene. Further, it is also an interesting exercise to probe the effect of the position of fluorine relative to that of the acetylenic moiety on the intermolecular structures in water complexes.

* To whom correspondence should be addressed. E-mail: naresh@chem.iitb.ac.in.

10.1021/jp809121n CCC: $40.75
Published on Web 02/10/2009

2. Methods

A. Experimental. The details of the experimental setup have been described elsewhere.[6] Briefly, helium buffer gas at 4 atm was bubbled through a mixture of 4FPHA (Aldrich)/2FPHA (Aldrich) and water kept at room temperature and expanded through a 0.5-mm-diameter pulsed nozzle (Series 9, Iota One; General Valve Corporation). The electronic excitation was achieved using a frequency-doubled output of a tunable dye laser (Narrow Scan GR; Radiant Dyes) pumped with second harmonic of a Nd:YAG laser (Surelite I-10; Continuum). The fluorescence excitation spectra were recorded by monitoring the total fluorescence with a photomultiplier tube (9780SB+1252-5F; Electron Tubes Limited) and a filter (WG-320) combination, while scanning UV laser frequency. The IR spectrum of the complex was obtained using fluorescence dip infrared (FDIR) spectroscopic method.[7] In this method, the population of a target species was monitored by the fluorescence intensity following its electronic excitation to the $S_1 \leftarrow S_0$ origin band with a UV laser pulse. A tunable IR laser pulse was introduced 100 ns before the UV laser pulse. When the IR frequency was resonant with the vibrational transition of the target species, the ground-state population decreased, resulting in the depletion of the fluorescence signal. Further, to separate out the transitions belonging to various species present in the LIF excitation spectrum, IR-UV hole-burning spectroscopy was also carried out. In this technique, a LIF excitation spectrum was recorded for the region of interest. Next, an IR pulse was tuned to a vibrational transition of a specific species of interest, while a delayed tunable UV laser probed the $S_1 \leftarrow S_0$ transition region. In the event of the UV laser being resonant with the transition of the same species to which the IR pulse was tuned to, the fluorescence intensity decreased in comparison with the first spectrum. The lowering of the intensity in the second spectrum relative to that of the first one allowed identification of relevant transitions. In our experiments, the source of tunable IR light was an idler component of a $LiNbO_3$ OPO (Custom IR OPO; Euroscan Instruments) pumped with an injection-seeded Nd:YAG laser (Briliant-B; Quantel). The IR OPO was calibrated by recording the photoacoustic spectrum of ambient water vapor. The typical bandwidth of both UV and IR lasers was about 1 cm^{-1}, and the absolute frequency calibration was within ± 2 cm^{-1}.

B. Computational. To supplement the experimental observations, we carried out ab initio calculations using the Gaussian 03 package.[8] The equilibrium structures of the monomers and various binary complexes were calculated at MP2(FC) and DFT-MPW3LYP methods using the aug-cc-pVDZ basis set. The nature of the stationary points obtained was verified by calculating the vibrational frequencies at the same level of theory. The stabilization energies were corrected for the zero point vibrational energy (ZPVE). One hundred percent of BSSE correction is believed to often underestimate the interaction energy, and 50% correction is a good empirical approximation. Therefore, we report the stabilization energies with 0, 50, and 100% BSSE correction.[9] The calculated symmetric and antisymmetric O−H stretching frequencies of water molecule at the MP2(FC)/aug-cc-pVDZ level were 3805 and 3940 cm^{-1}, respectively. However, the corresponding experimental values were 3657 and 3756 cm^{-1}. The scaling factor of 0.957 was devised by taking the ratio of the average experimental frequencies (3706 cm^{-1}) to the average calculated frequencies (3873 cm^{-1}).[10] Similarly, for the MPW3LYP/aug-cc-pVDZ level of theory a scaling factor of 0.9625 was devised. For a given method the same scaling factor was used for both C−H and O−H stretching frequencies for all the complexes reported here. The scaling factor was intended to correct for the basis set truncation, partial neglect of the electron correlation, and harmonic approximation. The calculated and scaled vibrational frequencies were then compared with the experimentally observed values.

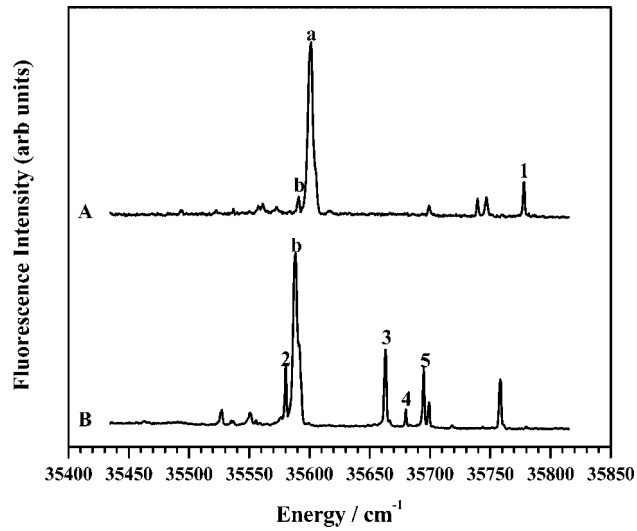

Figure 1. Fluorescence excitation spectrum of (A) 4FPHA and (B) 2FPHA in the presence of water. The peaks marked with "a" and "b" correspond to the band origin transitions 4FPHA and 2FPHA monomers, respectively. The transitions marked 1−5 are due to various water complexes. Both the spectra were recorded under identical experimental conditions.

3. Results

A. Spectra. The fluorescence excitation spectra of 4FPHA and 2FPHA in the presence of water are shown in Figure 1. There are no previous reports on the electronic spectra of both 4FPHA and 2FPHA, and in each case the most intense band can be assigned to the band origin of the $S_1 \leftarrow S_0$ electronic excitation. The band origin transitions for 4FPHA and 2FPHA appear at 35 601 and 35 588 cm^{-1}, respectively, while the corresponding transition for PHA is at 35 876 cm^{-1}.[4] The band origin transitions of 4FPHA and 2FPHA are shifted to the red by 275 and 288 cm^{-1}, respectively, relative to PHA. Further, it was also found that that 4FPHA contained trace impurity of 2FPHA, which results in the weak transition observed in the fluorescence excitation spectrum of 4FPHA. The fluorescence excitation spectrum of 4FPHA (Figure 1A) shows few transitions in the region 35 600−35 800 cm^{-1}. On the other hand, the fluorescence excitation spectrum of 2FPHA (Figure 1B) shows several transitions in the same energy region. The transitions marked 1−5 in the two spectra correspond to various water complexes (vide infra). The transition marked "1" in Figure 1A corresponds to the 4FPHA−H_2O complex, which is shifted by +177 cm^{-1}, relative to bare 4FPHA. In sharp contrast, the transitions marked with "2" and "3" correspond to two different 2FPHA−H_2O complexes, which are shifted by −8 and +75 cm^{-1}, relative to bare 2FPHA. Comparison of the shifts in the electronic transitions for the binary complexes of 4FPHA and 2FPHA with water indicates that the intermolecular structures might be different in each case. Further, the peaks marked with "4" and "5" in Figure 1B correspond to 2FPHA−$(H_2O)_2$ complexes (vide infra). These two transitions are shifted by +92 and +107 cm^{-1}, relative to bare 2FPHA.

The IR spectra of 4FPHA, 2FPHA, and their water complexes were recorded in the acetylenic C−H and the O−H stretching

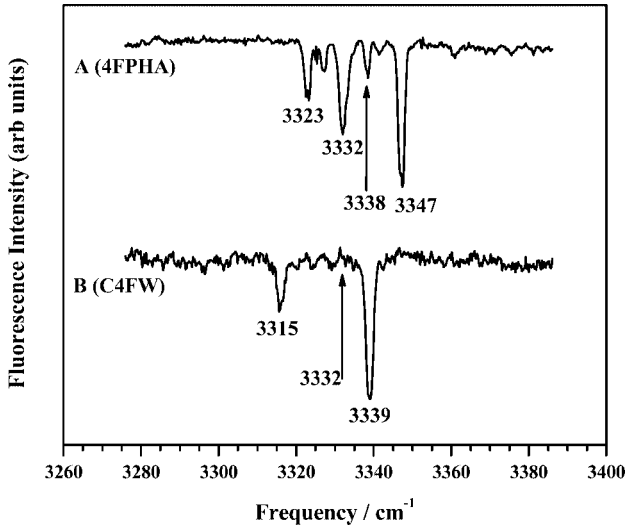

Figure 2. FDIR spectrum of (A) 4FPHA and (B) 4FPHA−H_2O (band-1) in the acetylenic C−H stretching region. In each spectrum, the arrow indicates the position of the centroid of observed transitions.

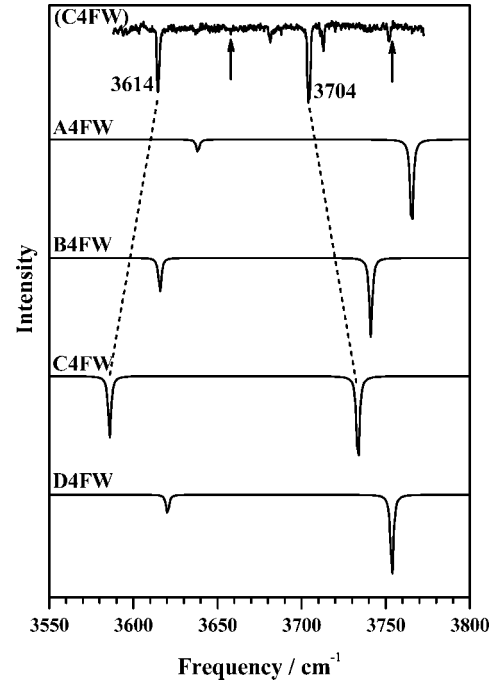

Figure 3. FDIR spectrum of the 4FPHA−H_2O complex in the O−H stretching region. The arrows indicate the positions of symmetric (3657 cm^{-1}) and antisymmetric (3756 cm^{-1}) stretching frequencies of the bare water molecule. Also presented are the simulated vibrational spectra for complexes **A4FW**−**D4FW**.

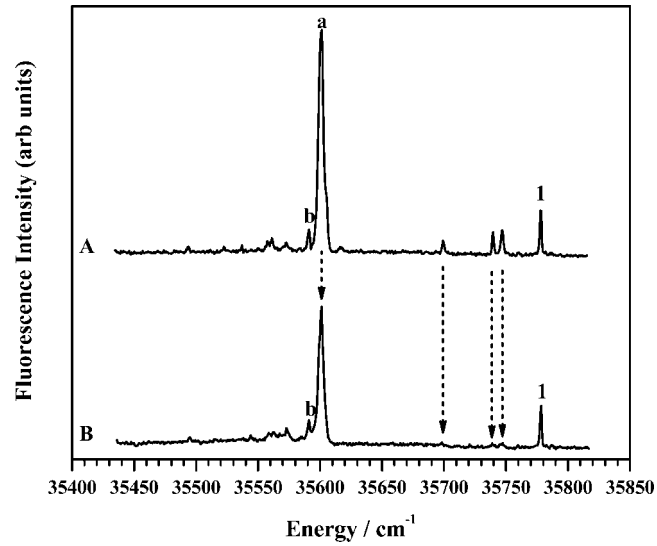

Figure 4. (A) Fluorescence excitation of 4FPHA in the presence of water. (B) IR-UV hole-burnt spectrum 4FPHA, which was recorded by pumping the acetylenic C−H stretching vibration with an IR laser fixed at 3347 cm^{-1} before the exciting UV laser. The arrows point to the bands with reduced intensities in the hole-burnt spectrum. The peaks marked with "a", "b", and "1" correspond to the band origin transitions of 4FPHA, 2FPHA, and 4FPHA−H_2O, respectively.

regions using the FDIR method by monitoring the fluorescence following excitation at their corresponding bands observed in the fluorescence excitation spectra while scanning the IR laser frequency. Figure 2A shows the FDIR spectrum of bare 4FPHA in the acetylenic C−H stretching region, in which three prominent bands appear at 3323, 3332, and 3347 cm^{-1}. The appearance of this spectrum is very similar to the corresponding spectrum of PHA and is indicative of the presence of Fermi resonance.[4,11] The FDIR spectrum of 4FPHA−H_2O complex, depicted in Figure 2B, consists of two transitions at 3315 and 3339 cm^{-1}. The appearance of this spectrum in terms of number of bands, band positions, and relative intensities is different from that of bare 4FPHA (Figure 2A). The difference in the two spectra clearly indicates the changes in the Fermi resonance couplings induced by interaction of H_2O with 4FPHA. To understand the nature of the interaction of water with 4FPHA, the FDIR spectrum of 4FPHA−H_2O complex was also recorded in the O−H stretching region, and the results are presented in Figure 3. The two strong bands appearing at 3614 and 3704 cm^{-1} arise because of the two O−H oscillators of the water moiety. Apart from two strong transitions, three weak transitions at 3681, 3713, and 3752 cm^{-1} were also observed in the spectrum. These three transitions can be assigned to the combination bands of intermolecular modes over the O−H stretching vibrations. Such combination bands have also been reported for several other binary complexes.[12] The FDIR spectrum of 4FPHA was also recorded in the O−H stretching region, which as expected did not show any transitions.

The fluorescence excitation spectrum of 4FPHA in the presence of water shows quite a few numbers of transitions. To assign the origin of these transitions and to check for the possibility of existence of isomers, IR-UV hole-burning spectroscopy was carried out, and the results are presented in Figure 4. Trace A shows the fluorescence excitation spectrum of 4FPHA in the presence of water, which is identical to the spectrum shown in Figure 1A. Trace B is the IR-UV hole-burnt spectrum, which was recorded by tuning the IR laser to pump the C−H vibrational transition of 4FPHA at 3347 cm^{-1} (Figure 2B), 100 ns before the exciting UV pulse, while scanning the UV laser. The IR-UV hole-burnt spectrum shows dips for all the observed transitions in the fluorescence excitation spectrum; however, the transitions marked "b" and "1" are the exceptions. As discussed earlier, the transition marked with "b" is the band origin of 2FPHA, which appears because of trace impurity of 2FPHA in 4FPHA.[13] This leaves the lone transition "1", which is due to 4FPHA−H_2O and confirms the presence of a single isomer of complex between 4FPHA and water.

The FDIR spectra of 2FPHA and 2FPHA−H_2O complexes in the acetylenic C−H stretching region are shown in Figure 5. The FDIR spectrum of 2FPHA shows an intense transition at 3334 cm^{-1}, accompanied by two weak transitions at 3318 and 3341 cm^{-1}. This observed spectrum is quite in contrast to the

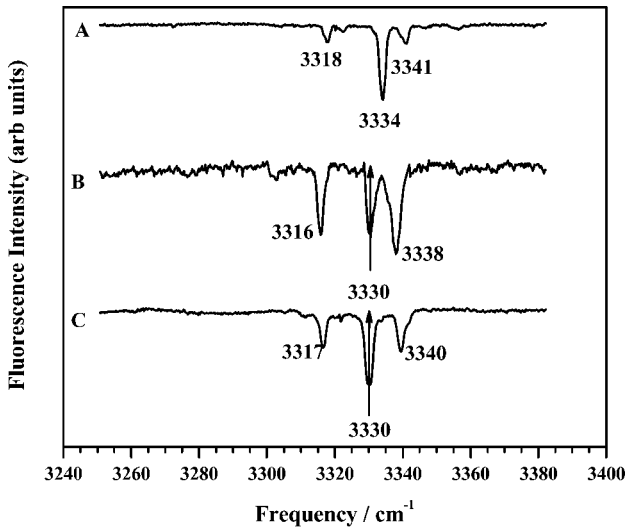

Figure 5. FDIR spectrum of (A) 2FPHA, (B) 2FPHA−H_2O (band-2), and (C) 2FPHA−H_2O (band-3) in the acetylenic C−H stretching region. The arrows indicate the position of the centroid of observed transitions.

corresponding spectra of PHA and 4FPHA, which indicate weakening of the Fermi mixing in 2FPHA. It is therefore reasonable to assume that the strong transition observed at 3334 cm^{-1} predominantly has the C−H stretching character and therefore can be assigned to the C−H stretching frequency of the acetylenic moiety. Figure 5B shows the FDIR spectrum of band-2 (Figure 1B), which is shifted by −8 cm^{-1} relative to the bare 2FPHA. This spectrum was recorded on the red edge of this band to minimize the interference from the bare 2FPHA, resulting in lower signal-to-noise ratio. Surprisingly, three intense transitions at 3316, 3330, and 3338 cm^{-1} were observed in this case. Similarly, the FDIR spectrum of band-3, which is depicted in Figure 5C, also shows three bands at 3317, 3330, and 3340 cm^{-1}. The appearance of three strong transitions in the FDIR spectra of 2FPHA−H_2O complexes (Figure 5B, C) can be assigned to the reappearance of Fermi resonance bands in 2FPHA due to interaction with water. Further, a careful inspection of all three spectra depicted in Figure 5 reveals that the weak satellite bands observed for the 2FPHA monomer gain intensity because of interaction with water, albeit with marginal changes in the peak positions. Because it is now fairly well established for phenylacetylene that the observed bands in the acetylenic C−H stretching region are due to Fermi resonance,[4,6,11] we assigned the bands observed in the FDIR spectra of 2FPHA−H_2O complexes in the acetylenic C−H region to be originating from Fermi resonance interaction. The FDIR spectra of the two 2FPHA−H_2O complexes in the O−H stretching region are depicted in Figure 6. The FDIR spectrum of band-2 is shown in Figure 6A, which consist of two transitions at 3618 and 3705 cm^{-1}. The appearance of this spectrum is very similar, in terms of both band positions and intensities, to that observed for the 4FPHA−H_2O complex (Figure 3). On the other hand, the FDIR spectrum of band-3, which is shown in Figure 6B, has two transitions appearing at 3636 and 3710 cm^{-1}.

IR-UV hole-burning spectroscopy was carried out, once again, to ascertain the origin of several transitions appearing in the 2FPHA−water system. Figure 7A shows the fluorescence excitation spectrum of 2FPHA in the presence of water, which is identical to the spectrum shown in Figure 1B. Figure 7B shows the IR-UV hole-burnt spectrum, which was recorded by tuning the IR laser to pump the acetylenic C−H vibrational transition of bare 2FPHA at 3334 cm^{-1}. The transitions arising

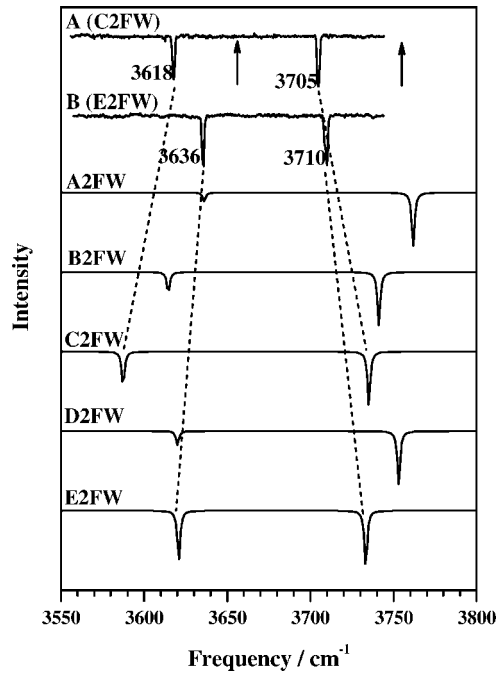

Figure 6. FDIR spectra of 2FPHA−H_2O complexes (A) band-2 and (B) band-3 in the O−H stretching region. The arrows indicate the positions of symmetric (3657 cm^{-1}) and antisymmetric (3756 cm^{-1}) stretching frequencies of the bare water molecule. Also presented are the simulated vibrational spectra for complexes **A2FW**−**E2FW**.

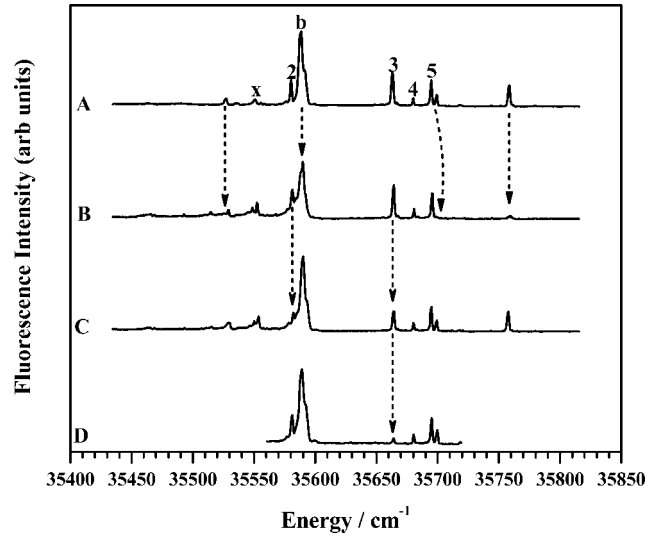

Figure 7. (A) Fluorescence excitation spectrum of 4FPHA in the presence of water. (B) IR-UV hole-burnt spectrum band-b, recorded by pumping the acetylenic C−H stretching vibration with an IR laser fixed at 3334 cm^{-1}. (C) IR-UV hole-burnt spectrum band-2, recorded by pumping the acetylenic C−H stretching vibration with an IR laser fixed at 3338 cm^{-1}. (D) IR-UV hole-burnt spectrum band-3, recorded by pumping the O−H stretching vibration with an IR laser fixed at 3710 cm^{-1}. The arrows in each case point to the dips corresponding to the transitions.

out of bare 2FPHA show diminished intensities, which are indicated by arrows. Shown in Figure 7C is the IR-UV hole-burnt spectrum of band-2 recorded by tuning the IR laser to its acetylenic C−H vibrational transition at 3338 cm^{-1}. Apart from lowering of the intensity of band-2, this spectrum also shows decrease in the intensity of band-3. This is because the IR spectra of band-2 and band-3 have an overlapping transition at 3338 cm^{-1}. To clearly separate transitions, the IR-UV hole-burnt spectrum of band-3 was recorded by pumping its O−H

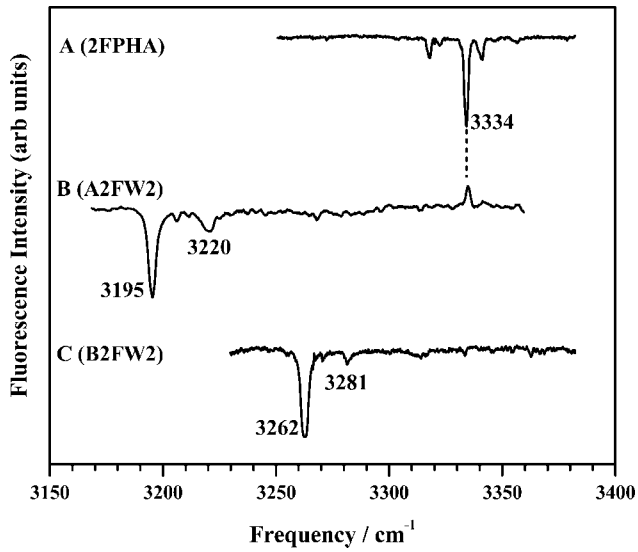

Figure 8. FDIR spectrum of (A) 2FPHA, (B) 2FPHA$-(H_2O)_2$ (band-4), and (C) 2FPHA$-(H_2O)_2$ (band-5) in the acetylenic C−H stretching region. In (B), the enhancement at 3334 cm^{-1} is due to the 2FPHA monomer.

stretching vibration at 3710 cm^{-1}, which is shown in Figure 7D. With these three IR-UV hole-burnt spectra, all but three transitions marked with "x", "4", and "5" have been accounted for. The transitions "4" and "5" arise out of two different isomers of 2FPHA$-(H_2O)_2$ and will be discussed below.[15] On the other hand, the band "x" does not show a transition either in the acetylenic C−H region or in the O−H stretching region, and therefore can be ruled out as a transition arising out of either bare 2FPHA or its water complex.

The FDIR spectra of bands "4" and "5" (Figure 1B) were recorded in the acetylenic C−H stretching region, and the results are presented in Figure 8. Also shown in Figure 8 is the FDIR spectrum of 2FPHA (trace A) for comparison. The FDIR spectrum of band-4, depicted in Figure 8B, shows an intense transition at 3195 cm^{-1}, along with a weak band at 3220 cm^{-1}. On the other hand, the FDIR spectrum of band-5 (Figure 8B) shows an intense transition at 3262 cm^{-1} along with a very weak band at 3281 cm^{-1}. In both cases, the stronger transitions can be assigned to the acetylenic C−H stretching vibrations of the complex and the weaker transition to a combination band of an intermolecular mode on the C−H stretching vibration. The acetylenic C−H stretching vibrations of bands "4" and "5" are shifted to a lower frequency by 139 and 72 cm^{-1}, respectively, relative to bare 2FPHA. This observation clearly indicates the formation of a C−H···O hydrogen-bonded complex, wherein the terminal acetylenic C−H group of 2FPHA interacts with the oxygen atom of a water molecule. The FDIR spectra in O−H stretching region for the bands "4" and "5" are shown in Figure 9. The FDIR spectrum of band-4 (Figure 9A) shows an intense transition at 3460 cm^{-1} along with three strong transitions at 3583, 3692, and 3696 cm^{-1} and a weak transition at 3535 cm^{-1}. The intensity of transition at 3460 cm^{-1} is much weaker than expected as the IR laser power is about one-fourth at this frequency in comparison with the rest of the tuning range in the O−H stretching region. The appearance of a transition at 3460 cm^{-1} is indicative of a strong water−water hydrogen bond.[14] This transition is accompanied by a combination band at 3535 cm^{-1}. The FDIR spectrum of band-5 (Figure 9B) shows an intense transition at 3541 cm^{-1}, which is indicative of a water−water hydrogen bond. The transitions at 3617, 3703, and 3739 cm^{-1} can be assigned to the remaining three O−H

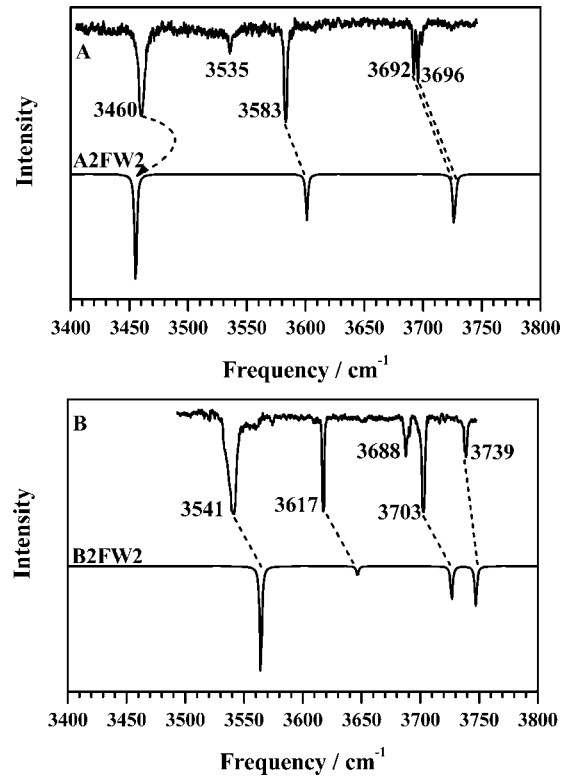

Figure 9. (A) FDIR spectrum of 2FPHA$-(H_2O)_2$ (band-4) presented along with the simulated vibrational spectrum of the **A2FW2** complex. (B) FDIR spectrum of 2FPHA$-(H_2O)_2$ (band-5) presented along with the simulated vibrational spectrum of the **B2FW2** complex.

oscillators, while the band at 3688 cm^{-1} can be assigned to a combination band on the basis of the comparison between the observed and the calculated spectra (vide infra). The appearance of an O−H stretching transition at 3739 cm^{-1} implies that the hydrogen bonding in one of the water molecules is either extremely weak or nonexistent.

B. Structures. To begin, water complexes of 4FPHA and 2FPHA were optimized starting from the corresponding PHA$-H_2O$ complexes. Further, several initial structures were generated by randomly placing the water molecule in the vicinity of the fluorine followed by geometry optimization. The MP2/aug-cc-pVDZ level calculations gave four minima on the potential energy hypersurface of 4FPHA$-H_2O$; these structures are depicted in Figure 10. Table 1 lists the ZPE- and BSSE-corrected stabilization energies. The first structure (**A4FW**) is a C−H···O "σ" hydrogen-bonded complex, wherein the lone pair on water acts as a hydrogen bond acceptor to the terminal acetylenic C−H group of 4FPHA, the structure of which is similar to the acetylene−water complex.[16] The ZPE- and 50% BSSE-corrected stabilization energy of this complex is 13.4 kJ mol^{-1}. In the second structure (**B4FW**) the O−H group of water molecule interacts with the π electron density of the benzene ring, leading to the formation of an O−H···π hydrogen-bonded complex, similar to the benzene−water complex.[17] The stabilization energy of **B4FW** is 13.8 kJ mol^{-1}. In the third structure (**C4FW**), both 4FPHA and water molecules act as donor and acceptor, leading to the formation of a quasi-planar cyclic complex. In this case, one of the O−H groups of water molecule is hydrogen-bonded to the π electron density of acetylenic C−C triple bond and the C−H group of the benzene ring in the ortho position is hydrogen-bonded to the oxygen atom of the water moiety. The structure of this complex is similar to that of the PHA−water complex and has the stabilization energy of 17.2

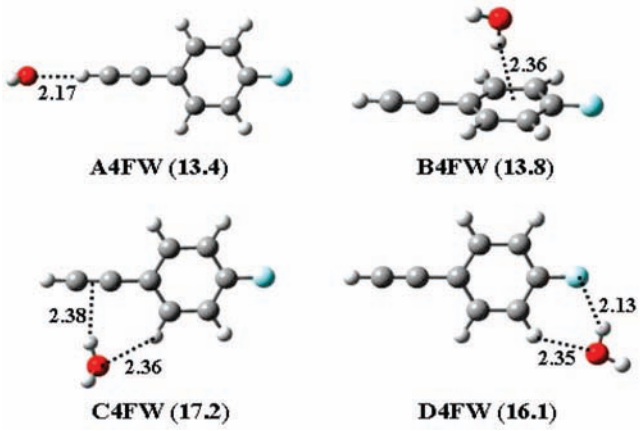

Figure 10. Structures of 4FPHA−H_2O complexes calculated at the MP2/aug-cc-pVDZ level. Distances are given in angstroms, and the 50% BSSE-corrected stabilization energies (kJ mol^{-1}) are shown in parentheses.

TABLE 1: ZPVE-Corrected Stabilization Energies (kJ mol^{-1}) for the Water Complexes of 4FPHA and 2FPHA Calculated at the MP2/aug-cc-pVDZ Level of Theory

	ΔE^a	ΔE^b	ΔE^c
A4FW	15.7	13.4	11.1
B4FW	18.5	13.8	9.1
C4FW	20.5	17.2	13.9
D4FW	18.8	16.1	13.4
A2FW	16.0	13.7	11.4
B2FW	19.3	14.4	10.4
C2FW	20.3	17.0	13.7
D2FW	19.1	16.5	13.8
E2FW	19.6	16.2	12.7

[a] No BSSE correction. [b] 50% BSSE correction. [c] 100% BSSE correction.

TABLE 2: Scaled Vibrational Frequencies and Their Shifts for 4FPHA−H_2O Complexes Calculated at the MP2/aug-cc-pVDZ Level of Theory[a]

	ν_{CH}	$\Delta\nu_{CH}$	ν_1	ν_3	$\Delta\nu_1$	$\Delta\nu_3$	$\Sigma\Delta\nu$
4FPHA	3331 (79)						
H_2O			3642 (4)	3771 (67)			
A4FW	3270 (343)	−61	3639(11)	3766 (80)	−3	−5	−8
B4FW	3329 (81)	−2	3616(53)	3742(122)	−26	−29	−55
C4FW	3324 (90)	−7	3586(93)	3734(140)	−56	−37	−93
D4FW	3331 (80)	0	3621(29)	3754(126)	−21	−17	−38

[a] The calculated intensities (km mol^{-1}) are shown in parentheses.

kJ mol^{-1}.[4a] The last structure (**D4FW**) comprises C−H···O and C−H···F hydrogen bonds, leading to formation of a six-membered cyclic complex, similar to the fluorobenzene−water and fluorostyrene−water complexes.[18,19] The **D4FW** complex has a stabilization energy of 16.1 kJ mol^{-1}. Surprisingly, the **A4FW** and **B4FW** complexes have lower stability in comparison with the two in-plane complexes, **C4FW** and **D4FW** with cyclic structures, with **C4FW** being the global minimum. Further, the C−H and O−H stretching vibrational frequencies of 4FPHA, H_2O, and various 4FPHA−H_2O complexes were also examined, and the values are listed in Table 2 along with their shifts.

A total of five stable minima were found for the 2FPHA−H_2O system, the structures of which are shown in Figure 11, and their stabilization energies are also listed in Table 1. The first four structures **A2FW**−**D2FW** have intermolecular structures similar to those of the corresponding 4FPHA−H_2O complexes. The stabilization energies of 2FPHA−H_2O complexes are

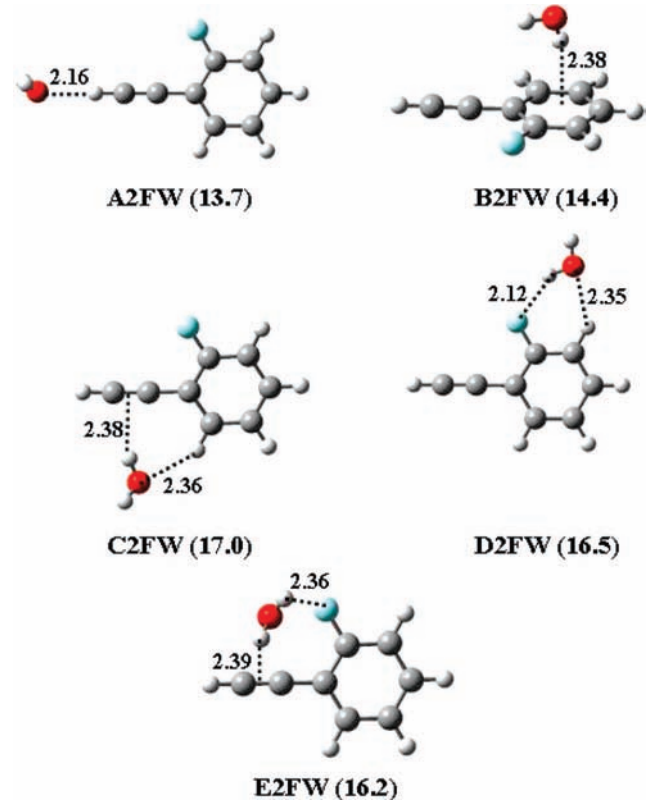

Figure 11. Structures of 2FPHA−H_2O complexes calculated at the MP2/aug-cc-pVDZ level. Distances are given in angstroms, and the 50% BSSE-corrected stabilization energies (kJ mol^{-1}) are shown in parentheses.

TABLE 3: Scaled Vibrational Frequencies and Their Shifts for 2FPHA−H_2O Complexes Calculated at the MP2/aug-cc-pVDZ Level of Theory[a]

	ν_{CH}	$\Delta\nu_{CH}$	ν_1	ν_3	$\Delta\nu_1$	$\Delta\nu_3$	$\Sigma\Delta\nu$
2FPHA	3332 (77)						
H_2O			3642 (4)	3771 (67)			
A2FW	3261 (358)	−71	3637(12)	3762 (79)	−5	−9	−14
B2FW	3330 (80)	−2	3615(49)	3737 (85)	−27	−34	−61
C2FW	3326 (87)	−6	3588(91)	3736(143)	−54	−35	−89
D2FW	3332 (78)	0	3621(33)	3754(126)	−21	−17	−38
E2FW	3327 (88)	−5	3621(53)	3734 (53)	−21	−37	−58

[a] The calculated intensities (km mol^{-1}) are shown in parentheses.

marginally (about 0.3−0.6 kJ mol^{-1}) higher than those of the corresponding 4FPHA−H_2O complexes, with the exception of **C2FW,** which is about 0.2 kJ mol^{-1} lower than the corresponding **C4FW** complex. This lowering can be attributed to the proximity of the fluorine to the acetylene moiety. The fifth 2FPHA−H_2O complex (**E2FW**) has a unique structure, wherein the water molecule forms a double-donor hydrogen-bonded structure. In **E2FW**, the two O−H groups of water molecule are hydrogen-bonded to fluorine atom and π electron density of C−C triple bond. This structure is a consequence of spatial proximity of the two functional groups. The stabilization energy of **E2FW** is 16.2 kJ mol^{-1}, marginally lower than that of **C2FW** and **D2FW**, but higher than that of **A2FW** and **B2FW**. Table 3 lists the calculated and scaled C−H and O−H stretching vibrational frequencies of 2FPHA and its water complexes along with their shifts.

Because of limitations in our computational resources, we calculated the structures of 2FPHA−$(H_2O)_2$ complexes using the DFT-MPW3LYP/aug-cc-pVDZ level of theory. To set the confidence limit for this level of theory, we recalculated all the

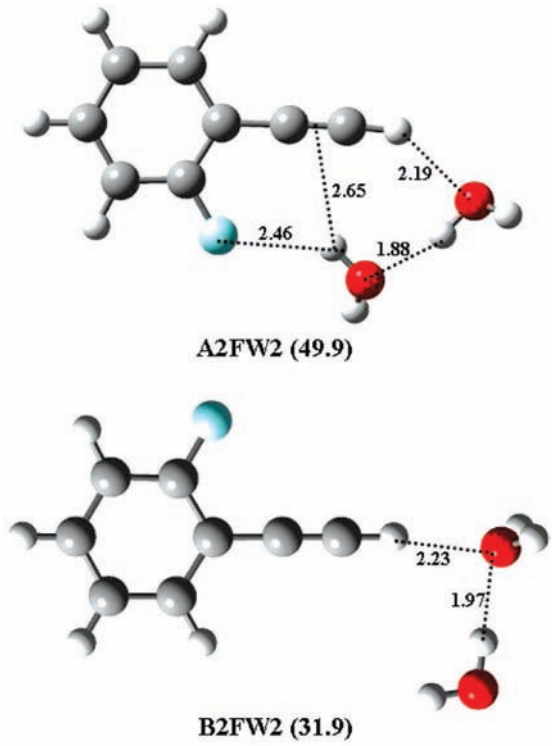

Figure 12. Structures of 2FPHA−$(H_2O)_2$ complexes calculated at the MPW3LYP/aug-cc-pVDZ level. Distances are given in angstroms, and the 50% BSSE-corrected stabilization energies (kJ mol^{-1}) are shown in parentheses.

structures and vibrational frequencies of 4FPHA−H_2O and 2FPHA−H_2O complexes. The results are presented and discussed in the Supporting Information. With the exception of O−H···π hydrogen-bonded complexes, wherein the O−H group of water molecule interacts with the π electron density, the stabilization energies calculated using the MPW3LYP/aug-cc-pVDZ level are comparable to those calculated using the MP2/aug-cc-pVDZ level of theory. For the complexes involving O−H···π interaction, the MPW3LYP/aug-cc-pVDZ level grossly underestimates the stabilization energies relative to the MP2/aug-cc-pVDZ level. This can be attributed to the large contribution of dispersion interaction to the stabilization energy. The FDIR spectra of 2FPHA−$(H_2O)_2$ complexes in the acetylenic C−H stretching region show substantial shifts to a lower frequency in the acetylenic C−H stretching vibration (Figure 8), which clearly indicates that these complexes involve hydrogen bonding between the acetylenic C−H group and oxygen atom on the water molecule. For this mode of interaction, calculations using the MPW3LYP/aug-cc-pVDZ level of theory yield stabilization energies comparable to those of the MP2/aug-cc-pVDZ level of theory. A large number of structural isomers can be expected for 2FPHA−$(H_2O)_2$ complexes. The FDIR spectra of both the 2FPHA−$(H_2O)_2$ complexes (bands "4" and "5") indicate the presence of linear C−H···O hydrogen bonding along with the H_2O−H_2O interaction. Starting with the **A2FW** structure, a second water molecule was added in various orientations and several initial structures were generated. The initial structures were then optimized using the MPW3LYP/aug-cc-pVDZ level of theory followed by vibrational frequency calculation. These optimization calculations converged onto two different minima; these structures are depicted in Figure 12. The stabilization energies are listed in Table 4, and the vibration frequencies along with their shifts are listed in Table 5. The first structure (**A2FW2**) is a cyclic complex incorporating four

TABLE 4: ZPVE-Corrected Stabilization Energies (kJ mol^{-1}) for the 2FPHA−$(H_2O)_2$ Complexes Calculated at the MPW3LYP/aug-cc-pVDZ Level of Theory

	ΔE^a	ΔE^b	ΔE^c
A2FW2	51.7	49.9	48.0
B2FW2	33.7	31.9	30.2

[a] No BSSE correction. [b] 50% BSSE correction. [c] 100% BSSE correction.

hydrogen bonds with stabilization energy of 49.9 kJ mol^{-1}. In **A2FW2**, the first water molecule apart from being a hydrogen bond acceptor to the acetylenic C−H group also acts as a hydrogen bond donor to the second water molecule. The second water molecule acts as hydrogen bond acceptor for the first water molecule. Additionally, one of the O−H groups of the second water molecule forms a bifurcated hydrogen bond with fluorine atom and π electron density of acetylenic C−C triple bond.[20] The structural motif of this complex is quite common and has been observed in several instances.[21] The second complex (**B2FW2**) has an unusual structure in which one water molecule adapts a double-acceptor structure forming hydrogen bonds with the acetylenic C−H group and O−H group second water molecule. With only two hydrogen bonds the stabilization energy of **B2FW2** is 31.9 kJ mol^{-1}, substantially lower than that of **A2FW2**.

4. Discussion

A. Structural Assignment. The vibrational spectra in the O−H stretching region were simulated for all the calculated complexes by convoluting a Lorentzian function of width (fwhm) 2 cm^{-1}. The agreement between the simulated and observed vibrational frequencies served as a benchmark for the structural assignment of various complexes. In the case of the water monomer, the experimentally observed two O−H stretching frequencies of the water molecule are at 3657 and 3756 cm^{-1}, corresponding to symmetric (ν_1) and antisymmetric (ν_3) stretching vibrations, respectively. In the event of hydrogen bond formation to one of the O−H groups of the water moiety, the two frequencies will now correspond to the hydrogen-bonded and free O−H stretching vibrations. Though only one of the O−H groups is involved in hydrogen bond formation, both stretching frequencies are lowered because of partial decoupling of the two O−H oscillators. The vibrational frequencies corresponding to the hydrogen-bonded and free O−H stretching vibrations are lower than those of the symmetric and antisymmetric stretching vibrations, respectively. Since both O−H stretching frequencies are lowered because of hydrogen bond formation, we used the total shift in the O−H stretching frequencies [$\Sigma(\Delta\nu) = (\Delta\nu_1 + \Delta\nu_3)$] as a tool to assign the intermolecular structures.[19]

The FDIR spectrum of 4FPHA in the acetylenic C−H stretching region, depicted in Figure 2A, is very similar to that observed for PHA and shows three prominent bands at 3323, 3332, and 3347 cm^{-1}.[4,11] Even in the case of PHA, three prominent transitions were observed at 3318, 3325, and 3343 cm^{-1}, of which the two higher energy transitions were assigned to be originating out of Fermi resonance between the acetylenic C−H oscillator with one quantum of C≡C stretch and two quanta of C−H out-of-plane bend, while the other weaker bands were assigned to the transitions arising out of higher order coupling terms.[11] We had earlier reported deperturbation analysis for PHA using a two-state Fermi resonance model for the two strong transitions observed at 3325 and 3347 cm^{-1}.[4,6] However,

TABLE 5: Scaled Vibrational Frequencies and Their Shifts for 2FPHA−$(H_2O)_2$ Complexes Calculated at the MPW3LYP/aug-cc-pVDZ Level of Theory[a]

	ν_{CH}	$\Delta\nu_{CH}$	ν_1	ν_2	ν_3	ν_4
2FPHA	3351 (100)					
H_2O			3654 (4)	3760 (62)		
A2FW2	3255 (323)	−96	3458 (410)	3602 (157)	3728 (136)	3729 (78)
B2FW2	3295 (350)	−56	3564 (247)	3647 (22)	3727 (81)	3747 (92)

[a] The calculated intensities (km mol^{-1}) are shown in parentheses.

in view of the observed complexity of the FDIR spectrum of 4FPHA, the two-state Fermi resonance model may not be completely appropriate. Since the primary goal of this work is to elucidate the structures of the water complexes on the basis of spectral signatures observed in the IR spectra, we used a relatively simple weighted-average model to analyze the IR spectra in the acetylenic C−H stretching region.[22] In the case of 4FPHA, the three transitions at 3323, 3332, and 3347 cm^{-1}, with relative intensities of 0.41, 0.63, and 1.0, respectively, give raise to centroid at 3338 cm^{-1}. Therefore, the unperturbed acetylenic C−H oscillator can be tentatively assigned to be occurring at 3338 cm^{-1}. The uncertainty in the band positions was less than 1 cm^{-1}, while the uncertainty in the band intensities was about 9−12%. We carried out the weighted average for several spectra, and the position of the centroid was found to be within 1 cm^{-1}. The FDIR spectrum of 4FPHA−H_2O complex, shown in Figure 2B, consists of two transitions at 3315 and 3339 cm^{-1}. The change in the appearance of this spectrum is indicative of changes in the Fermi resonance coupling in 4FPHA upon interaction with water. It is interesting to note that the FDIR spectrum of the 4FPHA−H_2O complex once again very is similar to the corresponding spectrum of the PHA−H_2O complex.[4] The centroid of the two transitions observed in the 4FPHA−H_2O complex can be estimated to be at 3332 cm^{-1}. This indicates that the acetylenic C−H stretching vibration of 4FPHA shifts by 6 cm^{-1} to a lower frequency upon interaction with H_2O. Since the appearance of Fermi resonance bands in 4FPHA involves C≡C and C−H oscillators, any perturbation of these two oscillators will lead to changes in the characteristics of the IR spectrum in the acetylenic C−H stretching region. Out of the four possible structures of the 4FPHA−H_2O complex, only two structures (**A4FW** and **C4FW**) incorporate the interaction between the water molecule and C≡C and/or C−H oscillators. However, the vibrational frequency calculations for the **A4FW** structure predict that the acetylenic C−H stretching vibration shifts by 61 cm^{-1} to a lower frequency because of the presence of C−H···O hydrogen-bonded interaction (Table 2), which is much larger in comparison with the experimentally observed shift of 6 cm^{-1}. Hence, this structure can be ruled out. Further, the calculated shift of 7 cm^{-1} in the C−H stretching frequency for the **C4FW** structure is in very good agreement with the experimentally estimated shift of 6 cm^{-1}. The FDIR spectrum of the 4FPHA−H_2O complex in the O−H stretching region is presented in Figure 3 along with the simulated spectra for various isomers of the 4FPHA−H_2O complex, and Table 2 lists all the vibrational frequencies along with their shifts. At first glance, it appears that the calculated spectra of the **B4FW**, **C4FW**, and **D4FW** structures are in reasonable agreement with the experimental spectrum. However, a closer inspection reveals that the simulated spectrum corresponding to **C4FW** matches well in terms of both band positions and intensities. Further, the two transitions in the FDIR spectrum appear at 3614 and 3704 cm^{-1}, representing a total shift in the O−H stretching frequencies [$\Sigma(\Delta\nu)$] of 95 cm^{-1}. From Table 2, it can be seen that the **C4FW** structure shows $\Sigma(\Delta\nu) = 93$ cm^{-1}, which is in excellent agreement with the experimental value. Additionally the **C4FW** structure is the global minimum for the 4FPHA−H_2O complex. Thus, the IR spectra in the acetylenic C−H stretching region and in the O−H stretching region and the stabilization energy clearly favor the formation of a quasi-planar cyclic complex **C4FW**, which is characterized by the presence of hydrogen bonding between the O−H group of water molecule with the π electron density of acetylenic C−C triple bond along with the hydrogen bond between the C−H group of benzene ring in the ortho position with the oxygen of the water moiety. The intermolecular structure of the 4FPHA−H_2O complex is similar to that of the PHA−H_2O complex.[4a]

The FDIR spectrum of 2FPHA in the C−H stretching region, shown in Figure 5A, surprisingly is dominated by single intense transition at 3334 cm^{-1}, suggesting the weakening of the Fermi resonance coupling relative to PHA and 4FPHA. Therefore, the intense transition is assigned to the acetylenic C−H stretching vibration. Surprisingly, both the 2FPHA−H_2O complexes, depicted in Figure 5B, C, show a marked increase in the Fermi resonance coupling. This behavior is a reversal to that observed in the case of PHA and 4FPHA, wherein interaction with water leads to diminishing of Fermi resonance coupling. The centroid of the three observed transitions in both the 2FPHA−H_2O complexes can be estimated to be at ∼3330 cm^{-1}, thereby shifting the C−H stretching vibration by −4 cm^{-1}, relative to the bare 2FPHA. As discussed earlier, in phenylacetylenes the appearance of Fermi resonance bands in the acetylenic C−H stretching region is due to the coupling of the C−H and C≡C oscillators. In the case of 2FPHA−H_2O complexes, the strengthening of Fermi resonance coupling, relative to bare 2FPHA, can be interpreted as the interaction of water molecule with the acetylenic moiety of 2FPHA. The structures of various 2FPHA−H_2O complexes are shown in Figure 11, and the two complexes **C2FW** and **E2FW** account for such an interaction. Figure 6 shows the comparison between the experimental and the simulated spectra of 2FPHA−H_2O complexes in the O−H stretching region. The FDIR spectrum of band-2 (Figure 6A) shows two transitions at 3618 and 3705 cm^{-1}, which is almost identical to the FDIR spectrum of the 4FPHA−H_2O complex shown in Figure 3, with minor changes in peak positions. The experimentally observed $\Sigma(\Delta\nu)$ of 90 cm^{-1} is in excellent agreement with the calculated value of 89 cm^{-1} for the **C2FW** structure. Further, with **C2FW** being the global minimum, the band-2 can be unambiguously assigned to this structure. The FDIR spectrum of band-3 (Figure 6B) shows two transitions in the O−H stretching region at 3636 and 3710 cm^{-1}, with an effective $\Sigma(\Delta\nu)$ of 67 cm^{-1}. The comparison of calculated and experimental $\Sigma(\Delta\nu)$ values (Table 3) suggests that **B2FW** and **E2FW** are two possible structures. On the other hand, comparison of stabilization energies (Table 1) suggests that **D2FW** and **E2FW** are the two possible structures. However, the simulated spectrum of **E2FW** is in excellent agreement with the experimental spectrum in terms of both band positions and intensities. Moreover, from the FDIR spectrum of band-3 in the acetylenic C−H stretching region (Figure 5C), it is very

clear that water molecule interacts with the acetylenic moiety of 2FPHA, which is present only in **E2FW**. Therefore, band-3 can be unambiguously assigned to the **E2FW** structure.

The bands "4" and "5" observed in the fluorescence excitation spectrum of 2FPHA (Figure 1B) show a large shift in the acetylenic C−H stretching frequency of 139 and 72 cm^{-1}, respectively, relative to bare 2FPHA. This implies, in a straightforward manner, that these two complexes incorporate C−H···O hydrogen bonding, through the interaction of oxygen atom on one of the water molecule with the acetylenic C−H group. Comparison of experimental and simulated spectra for the two 2FPHA−$(H_2O)_2$ complexes in the O−H stretching region is presented in Figure 9. In both cases, the agreement between the calculated and the experimental spectra is reasonable.[14] Hence, the structures of the two observed 2FPHA−H_2O complexes were assigned to **A2FW2** (band-4) and **B2FW2** (band-5), respectively. Further, the appearance of 3739 cm^{-1} in the O−H stretching region of band-5 (Figure 9B) supports the assignment of band-5 to the **B2FW2** structure, since this transition can be assigned to the antisymmetric stretching vibration of the double-acceptor water moiety.[23] It must be pointed out here that the MPW3LYP/aug-cc-PVDZ calculations, for both the 2FPHA−$(H_2O)_2$ complexes, underestimate the C−H···O and H_2O−H_2O interactions.

B. Structural Implications. The structures of water complexes of 4FPHA and 2FPHA are very similar to that of the PHA−H_2O complex,[4a] wherein one of the O−H groups of water molecule interacts with the C−C triple bond of acetylenic moiety, resulting in formation of an O−H···π hydrogen bond. This π hydrogen bond is reinforced by the C−H···O hydrogen bonding between the C−H group of benzene in the ortho position and the oxygen of water molecule. Interestingly, unlike benzene−fluorobenzene and styrene−fluorostyrene pairs,[18,19] substitution of fluorine atom on PHA does not lead to change structure. If we consider the energy contribution due to the interaction of oxygen atom of the water moiety with the C−H group of benzene ring in the ortho position to be very similar in the **C4FW** and **D4FW** (and also in **C2FW** and **D2FW**) structures, then in the case of fluorophenylacetylenes the experimental observed water complexes clearly indicate that formation of O−H···π (π electron density of acetylenic C−C triple bond) hydrogen bond is favored over the formation of O−H···F hydrogen bonding. This implies that the present finding conflicts with the Legon−Millen rules, since formation of a π hydrogen bond is preferred over a σ hydrogen bond.[2] Further, it was also found that substitution of fluorine on benzene ring enhances the binding of water. The experimental $\Sigma(\Delta\nu)$ values for the O−H stretching vibrations in the water complexes of PHA, 4FPHA, and 2FPHA complexes are 60, 95, and 90 cm^{-1}, respectively. These values are consistent with the calculated stabilization energies of 11.3, 17.3, and 17.0 kJ mol^{-1} for the corresponding complexes. This is indeed surprising as both the total shift in the O−H stretching frequencies and the binding energies for the fluorinated PHAs are about one-and-a-half times that of the unsubstituted PHA. These results are in contrast to benzene−fluorobenzene and styrene−fluorostyrene complexes, wherein the difference in the binding energy of water to the unsubstituted and fluorinated molecule is only marginal.[9,18,19] The present experimental and theoretical results clearly indicate that substitution of fluorine atom reinforces the binding of water molecule to the π electron density of the acetylenic C−C triple bond instead of switching.

An interesting observation can be made for the shifts in the electronic transitions for the 4FPHA−H_2O (**C4FW**) and 2FPHA−H_2O (**C2FW**) complexes. In the case of the 4FPHA−H_2O complex, the electronic transition shift is by +177 cm^{-1}, while the corresponding value for the 2FPHA−H_2O complex is −8 cm^{-1}. These two water complexes show markedly different behavior in their electronic shifts even though their intermolecular structures are almost identical. Similar observations were made for the complexes of phenol with formic acid and acetic acid. Even though the intermolecular structures of both the complexes are almost identical, the electronic transitions of the phenol−formic acid complexes shift to the blue, while the corresponding transitions for the phenol−acetic acid complexes shift to the red.[24] Similarly, in the case of dihydrogen-bonded complexes of phenol with borane−dimethylamine and borane−trimethylamine the shifts in the electronic transitions do not directly correlate with the shifts in the O−H stretching frequencies of phenol and the resulting intermolecular structures.[25] These results clearly indicate that comparison of shifts in the electronic transitions of complexes involving two different chromophoric molecules may not be a good spectroscopic tool to deduce the similarities/dissimilarities in the intermolecular structures.

The second 2FPHA−H_2O complex (**E2FW**) has the double-donor structure, in which both the O−H groups of water act as hydrogen bond donors to fluorine atom and acetylene C−C triple bond. The existence of double-donor water molecules has been reported in large water clusters, which include $(H_2O)_6$, $(H_2O)_7$, and $K^+(C_6H_6)_n(H_2O)_n$ complexes.[26,27] However, in smaller clusters such observations are extremely sparse. This, however, is a possibility when two hydrogen bond accepting functionalities lie in the proximity and 2FPHA provides the opportunity for the water molecule to interact in a double-donor fashion.

The proximity of the two functional groups also plays a guiding role in the formation of the two observed 2FPHA−$(H_2O)_2$ complexes. A network of hydrogen bonds that bridges a donor site with an acceptor site, within a molecule, using more than one water molecules is a well-established binding motif. The structure **A2FW2** incorporates the recognizable binding motif adopted by bridging water molecules.[21] On the other hand, the **B2FW2** structure is rather unique in which one of the water molecule acts as a double-acceptor. The existence of a double-acceptor water moiety has been reported in large water cluster anions,[28] but in smaller water clusters appearance of a double-acceptor is almost nonexistent. Therefore, it is rather surprising to observe the double-acceptor **B2FW2** structure, even though its stabilization energy is about 18 kJ mol^{-1} higher in energy than that of the **A2FW2** structure. With the much lower binding energy, the **B2FW2** is expected to be thermodynamically unfavorable over **A2FW2**, and at temperatures lower than 300 K, the population of **B2FW2** should be negligibly low. However, the observed intensity of the electronic transition corresponding to the **B2FW2** structure (band-5) in the fluorescence excitation spectrum (Figure 1B) is much higher than the transition corresponding to the **A2FW2** structure (band-4). The **B2FW2** structure is a stable minimum and forms during the initial phase of supersonic expansion. However, if the barrier for its interconversion to the most stable minimum **A2FW2** is sufficiently high then the 2FPHA−$(H_2O)_2$ complex is trapped in the higher energy minimum, which in the present case is **B2FW2**.[29] The observation of higher-energy **B2FW2** in the present experimental conditions can therefore be attributed to the kinetic trapping.

Conclusions

We investigated water complexes of 4FPHA and 2FPHA using IR-UV double resonance spectroscopic technique. The

band origin transitions for the $S_1 \leftarrow S_0$ electronic excitation of 4FPHA and 2FPHA occur at 35 601 and 35 588 cm^{-1}, respectively. The interaction of water with 4FPHA and 2PHA is very similar to that with PHA, which incorporates O−H···π and C−H···O interactions leading to the formation of a quasi-planar cyclic complex. The shifts in the O−H stretching frequencies and the stabilization energies point out that the binding of water to 4FPHA and 2FPHA is about 1.5 times stronger in comparison with that of PHA, even though the intermolecular structures are very similar. In the case of phenylacetylene, substitution of fluorine reinforces the interaction of water to the acetylenic C−C triple bond instead of switching to the fluorine site. Additionally, a second 2FPHA−H_2O complex was found, wherein the water forms a double-donor structure with the two O−H groups hydrogen-bonded to the π electron density of the C−C triple bond and the fluorine atom. This structure is a consequence of proximity of two acceptor functional groups. Two 2FPHA−$(H_2O)_2$ complexes were also observed, both of which incorporate C−H···O hydrogen bonding involving a terminal acetylenic C−H group. The global minimum for the 2FPHA−$(H_2O)_2$ complex is a structure in which a linear water dimer bridges the hydrogen bond donor and acceptor sites within 2FPHA. The second 2FPHA−$(H_2O)_2$ complex possesses an unusual structure with one of the water molecule acting as a double-acceptor. The appearance of this structure in our experiments is most likely due to the kinetic trapping.

Acknowledgment. We thank Prof. M. K. Mishra for his encouragement. This material is based upon work supported by the Department of Science and Technology (Grant No. SR/S1/PC/23/2008) and Board of Research in Nuclear Sciences (Grant No. 2004/37/5/BRNS/398) and Council of Scientific and Industrial Research (Grant No. 01(2268)/08/EMR-II). S.M. thanks UGC for the research fellowship.

Supporting Information Available: Tables listing the stabilization energies and the vibrational frequencies calculated for 4FPHA−H_2O and 2FPHA−H_2O complexes using the DFT-MPW3LYP/aug-cc-pVDZ level of theory. Also presented is the comparison of experimental and simulated spectra for the 4FPHA−H_2O and 2FPHA−H_2O complexes in the O−H stretching region. This material is available free of charge via the Internet at http://pubs.acs.org.

References and Notes

(1) (a) Etter, M. C. *Acc. Chem. Res.* **1990**, *23*, 120. (b) Etter, M. C. *J. Phys. Chem.* **1991**, *95*, 4601.

(2) Legon, A. C.; Millen, D. J. *Chem. Soc. Rev.* **1987**, *16*, 467.

(3) For example, see: Baures, P. W.; Rush, J. R.; Wiznycia, A. V.; Desper, J.; Helfrich, B. A.; Beatty, A. M. *Cryst. Growth Des.* **2002**, *2*, 653.

(4) (a) Singh, P. C.; Bandyopadhyay, B.; Patwari, G. N. *J. Phys. Chem. A* **2008**, *112*, 3360. (b) Singh, P. C.; Patwari, G. N. *J. Phys. Chem. A* **2008**, *112*, 4426. (c) Singh, P. C.; Patwari, G. N. *J. Phys. Chem. A* **2008**, *112*, 5121.

(5) Hernandez-Trujillo, J.; Vela, A. *J. Phys. Chem.* **1996**, *100*, 6524.

(6) Singh, P. C.; Patwari, G. N. *Curr. Sci.* **2008**, *95*, 469.

(7) Page, R. H.; Shen, Y. R.; Lee, Y. T. *J. Chem. Phys.* **1988**, *88*, 4621.

(8) Frisch, M. J.; Trucks, G. W.; Schlegel, H. B.; Scuseria, G. E.; Robb, M. A.; Cheeseman, J. R.; Montgomery, J. A., Jr.; Vreven, T.; Kudin, K. N.; Burant, J. C.; Millam, J. M.; Iyengar, S. S.; Tomasi, J.; Barone, V.; Mennucci, B.; Cossi, M.; Scalmani, G.; Rega, N.; Petersson, G. A.; Nakatsuji, H.; Hada, M.; Ehara, M.; Toyota, K.; Fukuda, R.; Hasegawa, J.; Ishida, M.; Nakajima, T.; Honda, Y.; Kitao, O.; Nakai, H.; Klene, M.; Li, X.; Knox, J. E.; Hratchian, H. P.; Cross, J. B.; Bakken, V.; Adamo, C.; Jaramillo, J.; Gomperts, R.; Stratmann, R. E.; Yazyev, O.; Austin, A. J.; Cammi, R.; Pomelli, C.; Ochterski, J. W.; Ayala, P. Y.; Morokuma, K.; Voth, G. A.; Salvador, P.; Dannenberg, J. J.; Zakrzewski, V. G.; Dapprich, S.; Daniels, A. D.; Strain, M. C.; Farkas, O.; Malick, D. K.; Rabuck, A. D.; Raghavachari, K.; Foresman, J. B.; Ortiz, J. V.; Cui, Q.; Baboul, A. G.; Clifford, S.; Cioslowski, J.; Stefanov, B. B.; Liu, G.; Liashenko, A.; Piskorz, P.; Komaromi, I.; Martin, R. L.; Fox, D. J.; Keith, T.; Al-Laham, M. A.; Peng, C. Y.; Nanayakkara, A.; Challacombe, M.; Gill, P. M. W.; Johnson, B.; Chen, W.; Wong, M. W.; Gonzalez, C.; Pople, J. A. Gaussian 03, revision A.1; Gaussian, Inc.: Wallingford, CT, 2004.

(9) Kim, K. S.; Tarakeshwar, P.; Lee, J. Y. *Chem. Rev.* **2000**, *100*, 4145.

(10) Carney, J. R.; Fedorov, A. V.; Cable, J. R.; Zwier, T. S. *J. Phys. Chem. A* **2001**, *105*, 3487.

(11) Stearns, J. A.; Zwier, T. S. *J. Phys. Chem. A* **2003**, *107*, 10717.

(12) (a) Patwari, G. N.; Ebata, T.; Mikami, N. *J. Chem. Phys.* **2002**, *116*, 6056. (b) Frost, R. K.; Hagemeister, F. C.; Arrington, C. A.; Schleppenbach, D.; Zwier, T. S. *J. Chem. Phys.* **1996**, *105*, 2065. (c) Robertson, W. H.; Kelley, J. A.; Johnson, M. A. *J. Chem. Phys.* **2000**, *113*, 7879.

(13) We had recorded the FDIR spectrum of the transition marked "b" in the fluorescence excitation spectrum of 4FPHA in the acetylenic C−H stretching region. This spectrum was found to be identical to that of 2FPHA shown in Figure 5A. Hence the assignment.

(14) Carney, J. R.; Hagemeister, F. C.; Zwier, T. S. *J. Chem. Phys.* **1998**, *108*, 3379.

(15) Ebata, T.; Mizuochi, N.; Watanabe, T.; Mikami, N. *J. Phys. Chem.* **1996**, *100*, 546.

(16) (a) Engdahl, A.; Nelander, B. *Chem. Phys. Lett.* **1983**, *100*, 129. (b) Peterson, K. I.; Klemperer, W. *J. Chem. Phys.* **1984**, *81*, 3842.

(17) (a) Engdahl, A.; Nelander, B. *J. Phys. Chem.* **1985**, *89*, 2860. (b) Wanna, J.; Menapace, J. A.; Bernstein, E. R. *J. Chem. Phys.* **1986**, *85*, 1795. (c) Suzuki, S.; Green, P. G.; Bumgarner, R. E.; Dasgupta, S.; Goddard, W. A., III.; Blake, G. A. *Science* **1992**, *257*, 942. (d) Pribble, R. N.; Garrett, A. W.; Haber, K.; Zwier, T. S. *J. Chem. Phys.* **1995**, *103*, 531. (e) Gutowsky, H. S.; Emilsson, T.; Arunan, E. *J. Chem. Phys.* **1993**, *99*, 4883.

(18) (a) Barth, H. D.; Buchhold, K.; Djafari, S.; Reimann, B.; Lommatzsch, U.; Brutschy, B. *Chem. Phys.* **1998**, *239*, 49. (b) Brutschy, B. *Chem. Rev.* **2000**, *100*, 3891.

(19) Singh, P. C.; Maity, S.; Patwari, G. N. *J. Phys. Chem. A* **2008**, *112*, 9702.

(20) (a) Head-Gordon, M.; Head-Gordon, T. *Chem. Phys. Lett.* **1994**, *220*, 122. (b) Duan, X.; Scheiner, S. *Int. J. Quantum Chem.* **1993**, *48* (S20), 181.

(21) (a) Watanabe, T.; Ebata, T.; Tanabe, S.; Mikami, N. *J. Chem. Phys.* **1996**, *105*, 408. (b) Zwier, T. S. *J. Phys. Chem. A* **2001**, *105*, 8827, and references therein.

(22) In the case of phenylacetylene, we had earlier used two-state deperturbation analysis that placed the unperturbed acetylenic C−H oscillator at 3334 cm^{-1} (see refs 4 and 6). On the other hand, analysis of the same spectrum using a weighted average model places the unperturbed acetylenic C−H oscillator at 3333 cm^{-1}. The accuracy of the centrod approach is about ± 1 cm^{-1}, relative to the two-state deperturbation model, which is within our experimental accuracy.

(23) Patwari, G. N.; Lisy, J. M. *J. Phys. Chem. A* **2003**, *107*, 9495.

(24) (a) Imhof, P.; Roth, W.; Janzen, C.; Spangenberg, D.; Kleinermanns, K. *Chem. Phys.* **1999**, *242*, 141. (b) Imhof, P.; Roth, W.; Janzen, C.; Spangenberg, D.; Kleinermanns, K. *Chem. Phys.* **1999**, *242*, 153.

(25) (a) Patwari, G. N.; Ebata, T.; Mikami, N. *J. Chem. Phys.* **2000**, *113*, 9885. (b) Patwari, G. N.; Ebata, T.; Mikami, N. *J. Chem. Phys.* **2001**, *114*, 8877.

(26) Pribble, R. N.; Zwier, T. S. *Science* **1994**, *265*, 75.

(27) Cabarcos, O. M.; Weinheimer, C. J.; Lisy, J. M. *J. Chem. Phys.* **1998**, *108*, 5151.

(28) (a) McCunn, L. R.; Headrick, J. M.; Johnson, M. A. *Phys. Chem. Chem. Phys.* **2008**, *10*, 3118. (b) Roscioli, J. R.; Hammer, N. I.; Johnson, M. A. *J. Phys. Chem. A* **2006**, *110*, 7517.

(29) Douberly, G. E.; Ricks, A. M.; Schleyer, P. v. R.; Duncan, M. A. *J. Chem. Phys.* **2008**, *128*, 021102.

JP809121N